Supplemental material

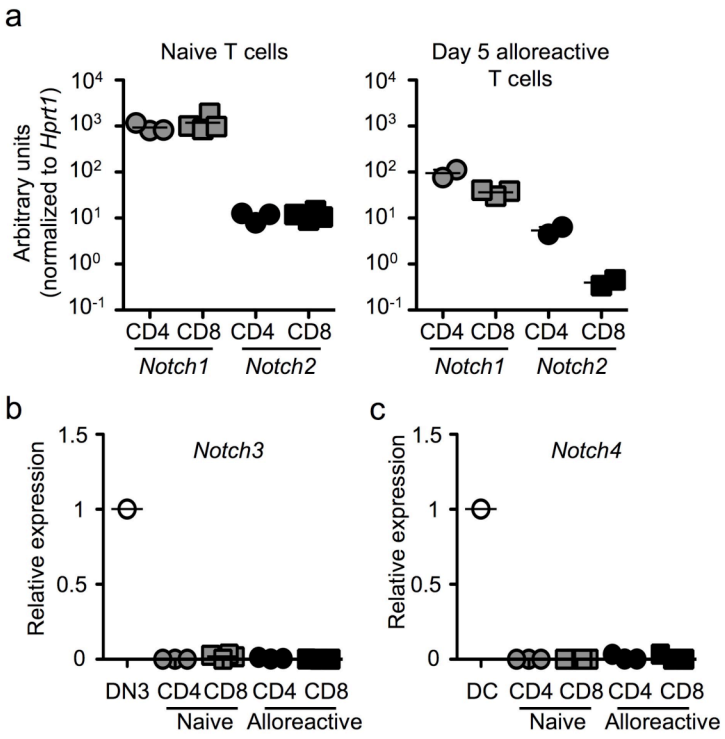

Figure S1. Expression of *Notch1* and *Notch2* mRNA and absence of detectable *Notch3/4* transcripts in naïve and alloreactive T cells.

Naïve $CD44^{low}CD62L^{hi}$ $CD4^+$ and $CD8^+$ T cells were sort-purified from B6 mice. Alloreactive T cells were purified as donor-derived $H2Kb^+H2Kd^-$ $CD4^+$ and $CD8^+$ T cells from the spleen of BALB/c allo-BMT recipient mice at day 5 after transplantation. Quantitative RT-PCR was performed. **(a)** Absolute quantification of *Notch1* and *Notch2* mRNA using a titration curve generated from known amounts of each PCR product. This allowed for direct comparison of *Notch1* and *Notch2* transcript abundance. Data are expressed as arbitrary units after normalization to *Hprt1* mRNA. **(b)** Relative quantification of *Notch3* transcripts using the ΔΔCt method. $Lineage^-CD44^{low}CD25^{hi}$ "double negative 3" (DN3) B6 thymocytes were used as a positive control for *Notch3* expression. **(c)** Relative quantification of *Notch4* transcripts using the ΔΔCt method. $I\text{-}A^{b+}CD11c^+$ spleen dendritic cells (DC) were used as a positive control for *Notch4* expression. Each symbol represents data obtained from one individual mouse. Relative rather than absolute quantification was performed in **(b)** and **(c)**, as *Notch3* and *Notch4* amplicons were not or only barely detectable in T cells.

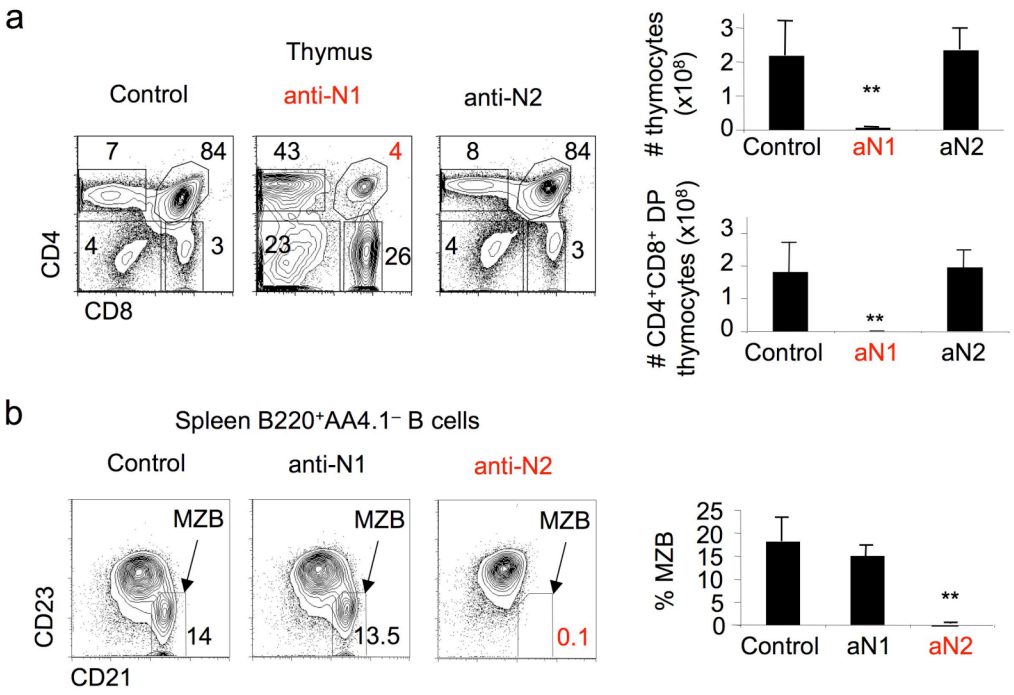

Figure S2. Anti-N1 and anti-N2 monoclonal antibodies block Notch signaling efficiently and specifically in vivo.

Adult B6 mice received anti-N1, anti-N2 or an isotype control antibody by i.p. injection (5 mg/kg, twice weekly for 2 weeks). On day 14, mice were euthanized for flow cytometric analysis of thymocytes and splenocytes. **(a)** Abundance of Notch1-dependent $CD4^{+}CD8^{+}$ double positive (DP) thymocytes. **(b)** Percentage of Notch2-dependent $CD21^{hi}CD23^{low}$ marginal zone B (MZB) cells among mature $B220^{+}AA4.1^{-}$ splenic B cells. Representative flow cytometry plots are shown. Numbers indicate the percentage of cells in each quadrant. Bar graphs represent mean +/– SD (n=3/group from one of three representative experiments). **p<0.01.

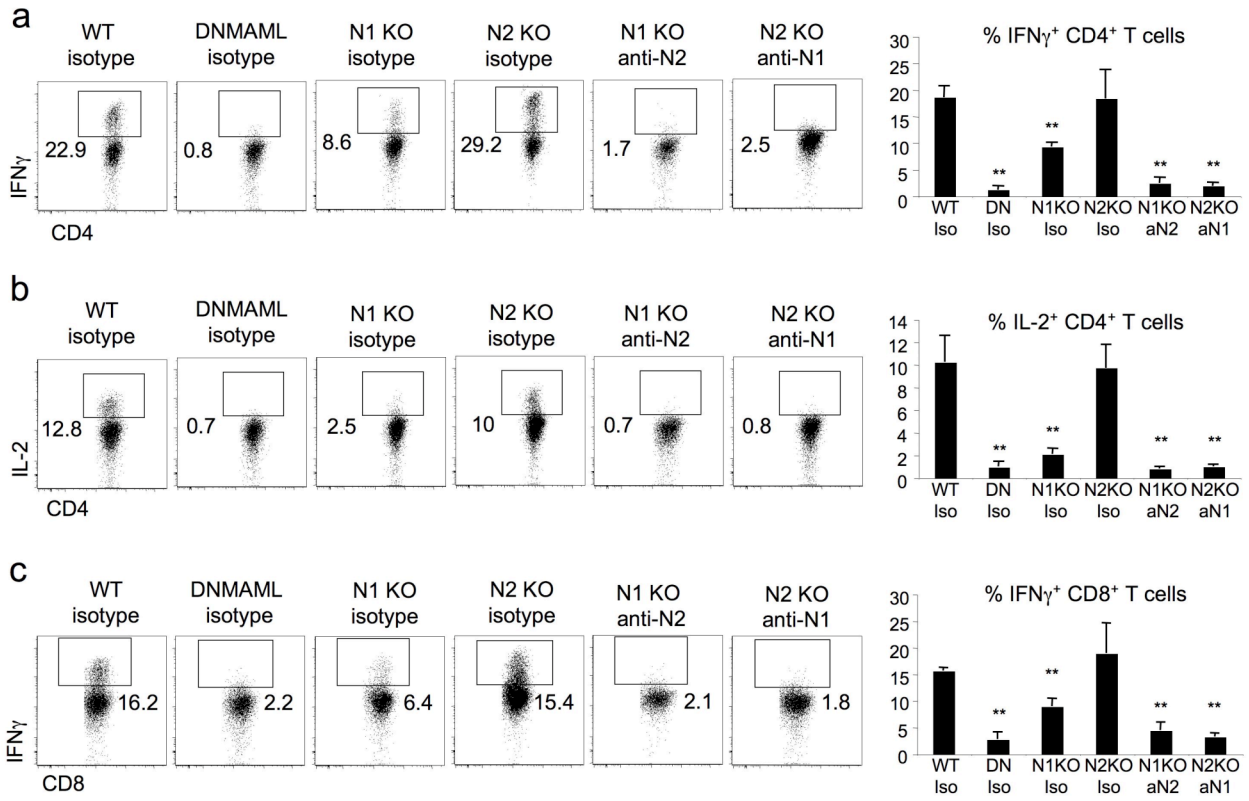

Figure S3. *Notch1* and *Notch2* exert cell-autonomous effects on cytokine production in alloreactive CD4$^+$ and CD8$^+$ T cells.

Lethally irradiated BALB/c mice (900 rads) were infused with TCD BM and WT, DNMAML, *Notch1$^{f/f}$ Cd4-Cre$^+$* (N1 KO) or *Notch2$^{f/f}$ Cd4-Cre$^+$* (N2 KO) spleen T cells. Isotype control, anti-Notch1 or anti-Notch2 monoclonal antibodies were administered i.p. as indicated (5 mg/kg, day 0 and day 3). At day 4.5, splenocytes were restimulated with plate-bound anti-CD3/CD28 antibodies followed by intracellular staining. **(a)** Percentage of IFNγ$^+$ cells among donor-derived H2Kb$^+$H2Kd$^-$ CD4$^+$ T cells; **(b)** Percentage of IL-2$^+$ cells among donor-derived CD4$^+$ T cells; **(c)** Percentage of IFNγ$^+$ cells among donor-derived CD8$^+$ T cells. Representative flow cytometry plots are shown. Numbers indicate the percentage of cells in each quadrant. Bar graphs represent mean +/– SD (n=3-5/group). **p<0.01.

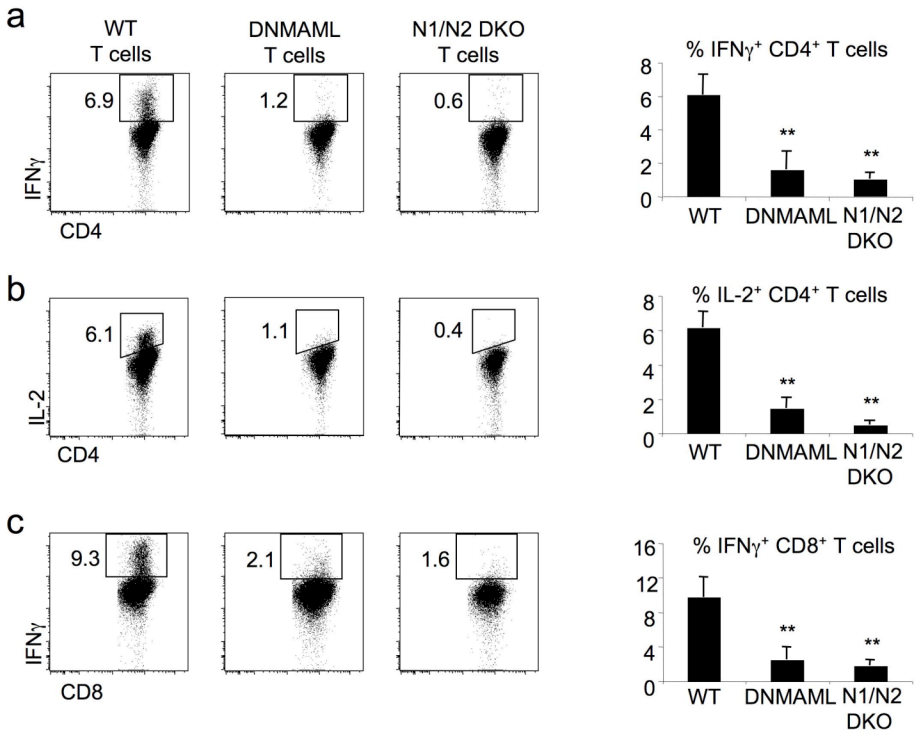

Figure S4. Combined *Notch1* and *Notch2* inactivation inhibits cytokine production to a similar extent as DNMAML expression in alloreactive T cells.

Lethally irradiated BALB/c mice (900 rads) were infused with TCD BM and WT, DNMAML or *Notch1*$^{f/f}$*Notch2*$^{f/f}$ *Cd4-Cre*$^{+}$ (N1/N2 DKO) spleen T cells. At day 5, splenocytes were restimulated with plate-bound anti-CD3/CD28 antibodies followed by intracellular staining. **(a)** % IFNγ^{+} cells in donor-derived H2Kb^{+}H2Kd^{-} CD4^{+} T cells; **(b)** % IL-2^{+} cells in donor-derived CD4^{+} T cells; **(c)** % IFNγ^{+} cells in donor-derived CD8^{+} T cells. Representative flow cytometry plots are shown. Numbers indicate the percentage of cells in each quadrant. Bar graphs represent mean +/– SD (n=4/group). **p<0.01.

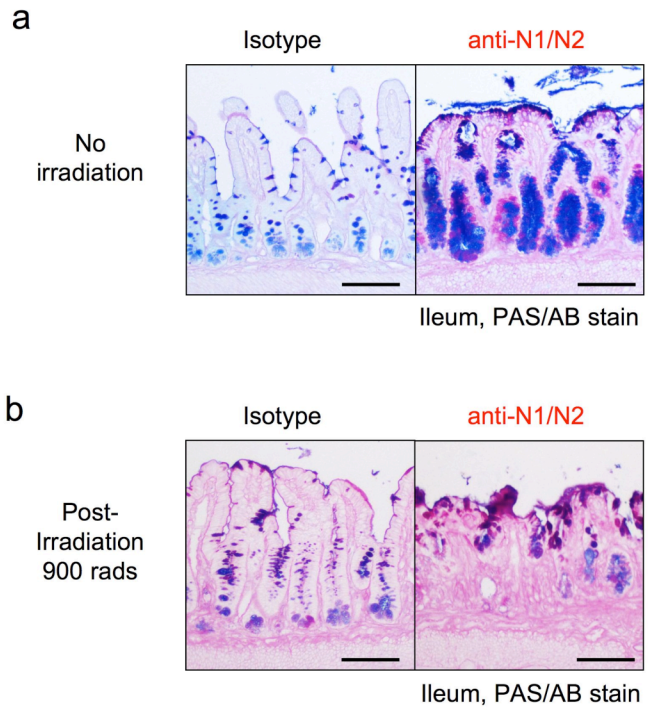

Figure S5. Differential effects of Notch blockade in the intestine in steady-state conditions and after bone marrow transplantation.

BALB/c mice were treated with anti-N1/N2 antibodies in steady-state conditions without irradiation (**a**) or after total body irradiation (900 rads) and transplantation of B6 TCD BM **(b)**. Periodic acid-Schiff/Alcian blue (PAS/AB) staining was used to identify goblet cells. As reported previously[24], Notch1/Notch2 inhibition led to massive goblet cell hyperplasia in steady-state conditions **(a)**. This was not seen after bone marrow transplantation, although the overall architecture of the intestinal epithelium was impaired by Notch blockade **(b)**.

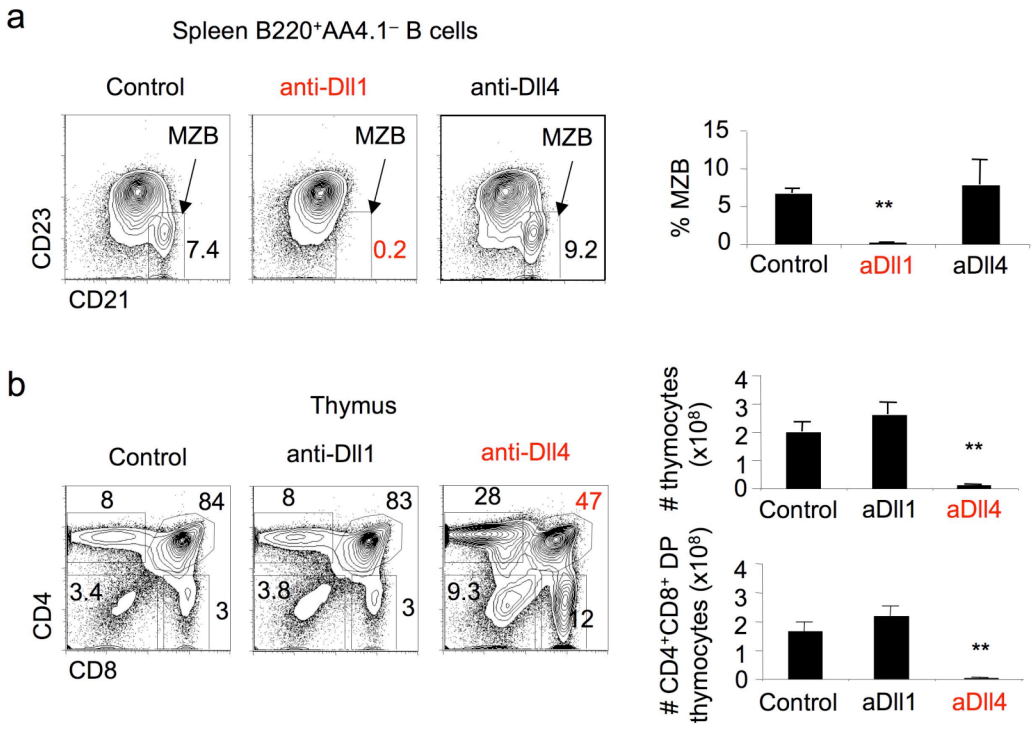

Figure S6. Anti-Dll1 and anti-Dll4 monoclonal antibodies block Notch ligands efficiently and specifically in vivo.

Adult B6 mice received anti-Dll1, anti-Dll4 or an isotype control antibody by i.p. injection (5 mg/kg, twice weekly for 2 weeks). On day 14, mice were euthanized for flow cytometric analysis of thymocytes and splenocytes. **(a)** Percentage of Dll1-dependent $CD21^{hi}CD23^{low}$ marginal zone B (MZB) cells among mature $B220^{+}AA4.1^{-}$ splenic B cells. **(b)** Abundance of Dll4-dependent $CD4^{+}CD8^{+}$ double positive (DP) thymocytes. Representative flow cytometry plots are shown. Numbers indicate the percentage of cells in each quadrant. Bar graphs represent mean +/– SD (n=3/group from one of three representative experiments). **p<0.01.

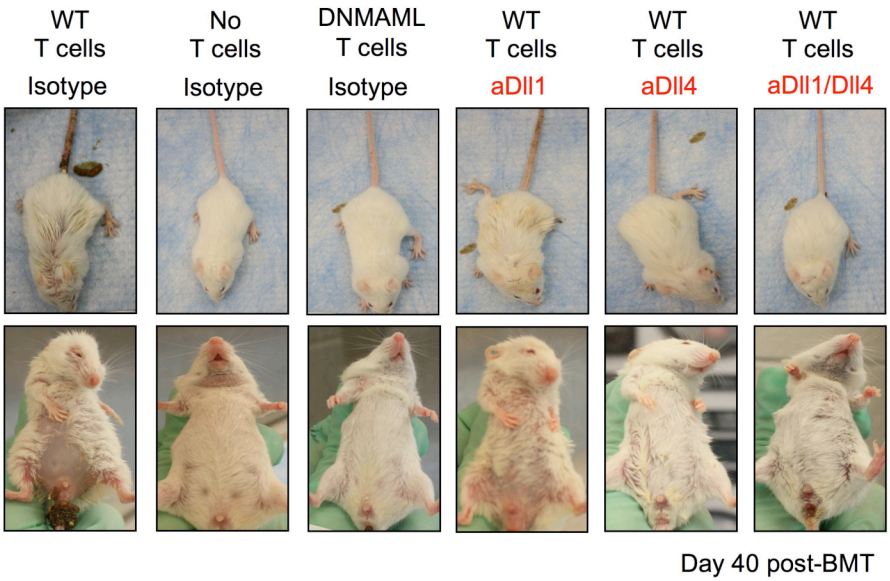

Figure S7. Representative examples of protection from clinical GVHD upon systemic Dll1/Dll4 blockade.

Lethally irradiated (850 rads) BALB/c mice were transplanted with TCD BM ($5x10^6$ cells), with or without WT or DNMAML T cells ($10x10^6$ splenocytes). Monoclonal antibodies were administered twice weekly as indicated (isotype control, anti-Dll1, anti-Dll4, anti-Dll1/Dll4). Pictures were taken at day 40 after transplantation.

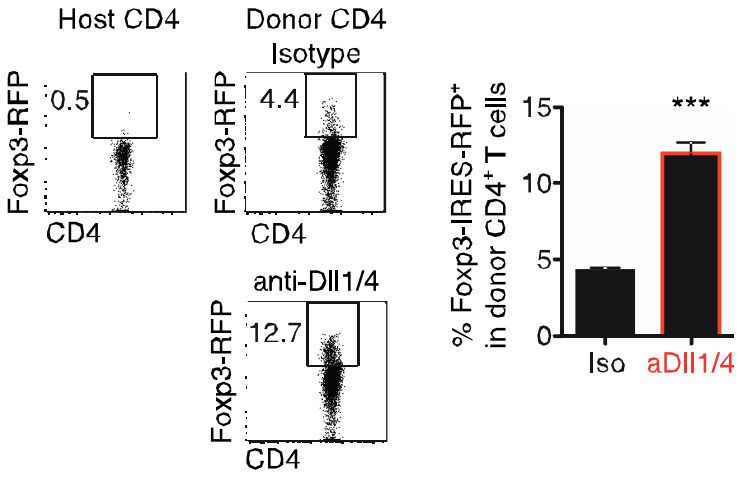

Figure S8. Increased accumulation of donor-derived FoxP3$^+$ CD4$^+$ T cells upon Dll1/Dll4 blockade after allo-BMT as revealed using a FoxP3-IRES-mRFP reporter allele.

Lethally irradiated BALB/c recipients (900 rads) were transplanted with TCD BM ($5x10^6$) and $5x10^6$ splenocytes from B6 FoxP3-IRES-mRFP reporter mice (expressing mRFP under control of endogenous *Foxp3* regulatory sequences). Isotype control or anti-Dll1/4 antibodies were administered biweekly. On day 11, mRFP fluorescence was studied by flow cytometry among H-2Kb$^+$ donor-derived CD4$^+$ T cells or in host CD4$^+$ T cells as a negative control.

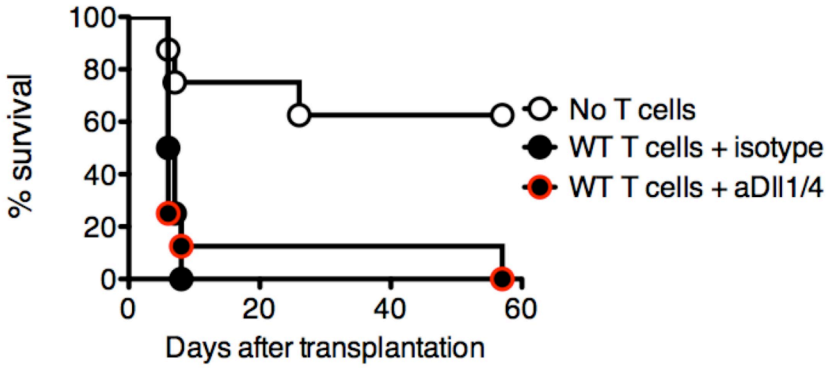

Figure S9. Splenocytes arising in anti-Dll1/Dll4-treated primary allogeneic transplant recipients do not transfer protection from GVHD in secondary recipients.

Lethally irradiated BALB/c recipients (900 rads) were transplanted with TCD BM ($5x10^6$) and $5x10^6$ B6 splenocytes. Isotype control or anti-Dll1/4 antibodies were administered biweekly (4 injections). On day 14, spleens from transplanted mice were harvested and mixed 1:1 (total of $12x10^6$ splenocytes) with splenocytes from naïve wild-type (WT) B6 mice. Secondary transplantation: lethally irradiated BALB/c mice (900 rads) received either B6 TCD BM alone ("no T cells"), naïve WT B6 splenocytes + alloreactive isotype control-treated WT splenocytes ("WT T cells + isotype") or naïve WT B6 splenocytes + alloreactive anti-Dll1/4-treated WT splenocytes ("WT T cells + aDll1/4) (n=8 mice/group). Recipients were monitored over time for survival and GVHD severity. There was no significant difference in survival between recipients of isotype control and anti-Dll1/Dll4-treated alloreactive splenocytes (p=0.895).

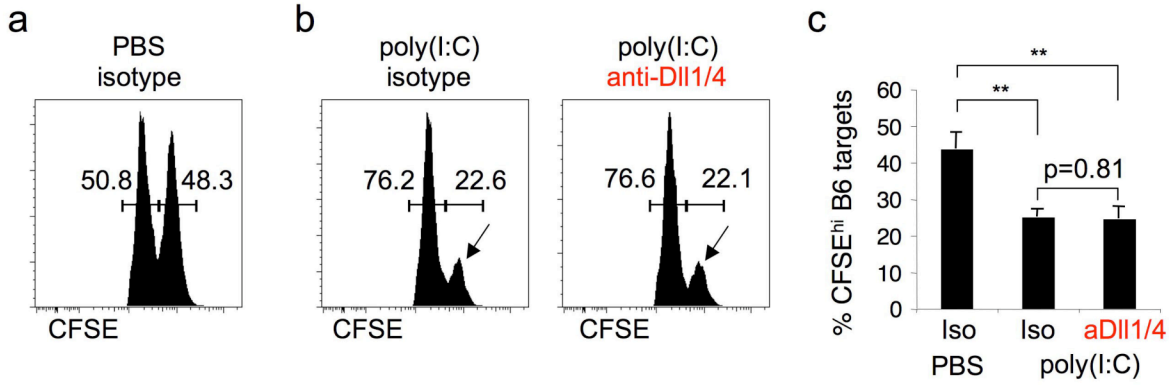

Figure S10. Dll1/Dll4 blockade does not impair alloresponsive NK cell function as revealed with an in vivo NK cell cytotoxicity assay.

BALB/c x B6 F1 mice (n=3/group) received istotype control antibodies or anti-Dll1/Dll4 antibodies at day -2. At day -1, mice were treated with PBS **(a)** or 200 μg poly(I:C) to activate NK cell effector function **(b)**. On day 0, mice received a 1:1 mixture of $CFSE^{low}$ F1 control splenocytes and $CFSE^{hi}$ BALB/c parental target splenocytes (6 x 10^6 each i.v.). Sixteen hours later, $CFSE^{+}$ cells were analyzed in the spleen by flow cytometry. Representative histograms are shown. Arrows point to $CFSE^{hi}$ BALB/c parental NK cell targets in poly(I:C)-treated mice; **(c)** Bar graph quantifying data presented in Figure S9a-b (mean +/- SD). Recovery of NK cell targets was significantly decreased in poly(I:C) as compared to PBS recipients, indicating efficient activation of NK cell function by poly(I:C) (**$p<0.01$). In vivo anti-hematopoietic NK cell cytotoxicity was not significantly different in mice treated with isotype control and anti-Dll1/Dll4 antibodies ($p=0.81$).

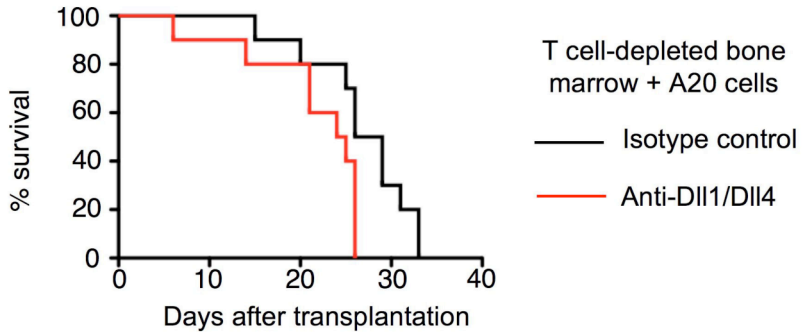

Figure S11. Anti-Dll1/Dll4 antibodies do not extend survival after T cell-depleted allo-BMT and challenge with host-type A20 tumor cells.

Lethally irradiated (900 rads) BALB/c mice were transplanted with TCD BM ($5x10^6$ cells) and A20-TGL host-type tumor cells (10^6). Monoclonal antibodies were administered twice weekly starting at day 0 for a total of four doses (isotype control vs. anti-Dll1/Dll4, n=10 mice/group). Progressive leukemia at the time of death was confirmed by necropsy or bioluminescence imaging in the majority of transplant recipients (Isotype control: 8/10 mice; anti-Dll1/Dll4: 7/10 mice).